

Spatially Resolved Single Bead Analysis: Homogeneity, Diffusion, and Adsorption in Cross-Linked Polystyrene**

Jörg Rademann,^{*[a]} Michael Barth,^[a] Roland Brock,^[a]
Hans-Joachim Egelhaaf,^[b] and Günther Jung^[a]

Abstract: Spatially resolved single bead analysis in the micrometer range was employed as a tool for evaluating homogeneity, diffusion, and adsorption in solid-phase supported reactions. Fluorescence microscopy (confocal and non-confocal) as well as IR microscopy were used to detect both the distribution of products and the formation of product gradients in representative reactions. For the first time, the optical slices of whole beads obtained by confocal fluorescence microscopy were compared with the fluorescence images of microtome-sliced beads. The experiments revealed that only physical slices of poly-

styrene beads deliver realistic representations of the distribution of fluorophores, and confirmed—in contrast to a recent report—the homogeneity of functional site distribution in polystyrene beads. Moreover, the pattern of product formation obtained from an acylation reaction as well as from an alkylation reaction were employed as probes to study the impact of bead size, diffusion, and adsorption on the reaction

progress. A simulation of the diffusion process was conducted and compared with the experimental results. Diffusional control was found neither in the case of the alkylation nor in the case of the acylation reaction under investigation. As a consequence, the reaction progress was not a function of the bead sizes as proposed in the literature. Interestingly, in the case of rhodamine acylation with substoichiometric amounts an adsorption-controlled reaction was found. This result highlights the significance of adsorptive effects in solid-phase supported chemistry.

Keywords: combinatorial chemistry
• fluorescence • IR spectroscopy •
solid-phase synthesis

Introduction

The advantages of multi-step solid-phase synthesis, such as simple isolation of intermediates by filtration, complete transformations by using high excess of reagents, and the feasibility of automated parallel and combinatorial synthesis, are evident.^[1, 2] However, as the understanding of solid-phase supported chemistry is still poor, decisions for a synthetic protocol development often rely rather on experience and routine than on scientifically validated knowledge.^[3–6]


Solid supports are characterized by the chemical and physical structure of the polymer. The structural parameters specifically determine each polymer–solvent–reagent system including swelling, polymer mobility, diffusion, and adsorption properties as well as the kinetics of solid-phase supported reactions. Single bead analysis and kinetic monitoring of solid-phase reactions were intensified during recent years.^[7–10] There are classical examples employing autoradiography to assess the quality of resin beads with elevated resolution.^[11, 12] However, this method has not been used to monitor reaction progress and is hardly generally applicable, due to the necessity of radioactive labelling. Thus, spatially and time-resolved single bead analysis using more accessible, optical microscopic techniques will enhance the knowledge on solid-phase reactions significantly. It will thus provide new opportunities for reaction monitoring and additional information for the rational design of improved resins for synthesis and other solid-phase applications.^[13, 14]

Results and Discussion

In this article we demonstrate the concept of spatially resolved single bead analysis employing fluorescence microscopy as well as IR microscopy. Three-dimensional represen-

[a] Dr. J. Rademann, Dipl.-Chem. M. Barth, Dr. R. Brock,
Prof. Dr. G. Jung
Institute of Organic Chemistry, University of Tübingen
Auf der Morgenstelle 18, 72076 Tübingen (Germany)
Fax: (+49) 7071-295560
E-mail: joerg.rademann@uni-tuebingen.de

[b] Dr. H.-J. Egelhaaf
Institute of Physical Chemistry, University of Tübingen
Auf der Morgenstelle 18, 72076 Tübingen (Germany)

 Supporting information for this article is available on the WWW under <http://wiley-vch.de/home/chemistry/or> from the author.

[**] Editorial note: For a similar study using confocal Raman spectroscopy, see the preceding paper by J. Kress, A. Rose, J. G. Frey, W. S. Brocklesby, M. Ladlow, G. W. Mellor, M. Bradley, *Chem. Eur. J.* **2001**, *7*, 3880–3883.

tations of resin beads can be obtained by methods of optical slicing.^[15, 16] In confocal microscopy a picture is generated by detecting the fluorescence light emitted from points of the object that are sequentially addressed by scanning a focussed laser beam of the excitation wavelength. Because of rejection of out-of-focus fluorescence by a delimiting aperture (pin-hole) in front of the detector optical slices of an object are obtained. Physical slicing followed by optical analysis is an alternative to optical slicing. It can be employed to collect information on the slices of a bead independently of the optical imaging characteristics of a microscope technique. With IR microscopy, on the contrary, it is possible to obtain spectra from whole resin beads in the transmission mode. All three approaches to spatial resolution in resin beads were pursued and compared.

Homogeneity of the functional site distribution: The homogeneity of the functional site distribution is a highly relevant parameter of resin beads in order to assure high loading and equal reactivity of all sites together with optimal site separation. Beads of cross-linked divinylbenzene (1%)-polystyrene (1 mmol g⁻¹, 200–400 mesh), which were aminomethylated subsequently to the polymerization step, were loaded with 5,6-carboxy-tetramethyl-rhodamine (CTMR) activated using tetramethyl-*O*-(benzotriazol-1-yl)-uronium tetrafluoroborate (TBTU) as the condensing agent. Swollen as well as non-swollen polymer beads were inspected with a confocal fluorescence microscope.^[17] Rhodamine-coupled

Abstract in German: *Räumlich aufgelöste Analytik von einzelnen Harzkugeln im Mikrometerbereich wurde durchgeführt, um die Homogenität, Diffusion und Adsorption von Festphasen-unterstützten Reaktionen zu untersuchen. Sowohl konfokale und nicht-konfokale Fluoreszenzmikroskopie als auch IR-Mikroskopie wurden benutzt, um die Produktverteilung und die Gradientenbildung in repräsentativen Beispielreaktionen nachzuweisen. Erstmals wurden optische Schnitte von ganzen Harzkugeln, die durch konfokale Fluoreszenzmikroskopie erhalten wurden, mit den Fluoreszenzbildern von Mikrotomschnitten verglichen. Die Experimente zeigten, dass nur die physikalischen Schnitte von Harzkugeln realistische Abbildungen der Produktverteilung lieferten und bestätigten – im Widerspruch zu einem kürzlich erschienenen Artikel – die homogene Verteilung der Reaktionszentren in Polystyrolkugeln. Darüber hinaus wurden die Muster der Produktbildung, die bei einer Acylierung bzw. bei einer Alkylierung erhalten wurden, als Sonde für den Einfluss von Kugelgröße, Diffusion und Adsorption auf den Reaktionsfortschritt eingesetzt. Eine Simulation des Diffusionsvorganges wurde durchgeführt und mit den experimentellen Ergebnissen verglichen. Diffusionskontrolle wurde dabei weder im Falle der untersuchten Alkylierung noch der Acylierung gefunden. Folglich war der Reaktionsfortschritt keine Funktion der Kugelgröße wie dies in der klassischen Literatur gefordert wird. Interessanterweise wurde bei der Acylierung mit Rhodamin mit substöchiometrischen Mengen ein Adsorptions-kontrollierter Reaktionsverlauf gefunden. Dieses Ergebnis unterstreicht die Bedeutung adsorptiver Effekte in der Festphasen-unterstützten Chemie.*

beads showed intense fluorescence at the surface, however, no fluorescence was detected at the interior of the optical slices (Figure 1 a,b). Recently, very similar images were

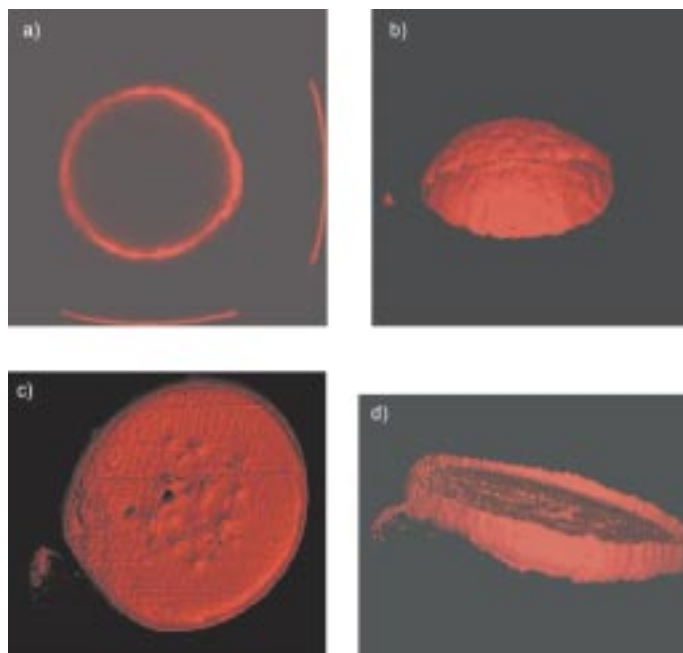


Figure 1. a, b) Typical beads of aminomethyl 1%-divinylbenzene-polystyrene (200–400 mesh, 1 mmol g⁻¹) acylated with CTMR (1 equiv) and inspected with confocal fluorescence microscopy; a) one optical slice, b) a three-dimensional reconstruction from several slices. c, d) Microtome cuts of CTMR-labelled resin beads. Reconstruction of several optical slices displays a physical bead slice of 5 µm thickness and 150 µm in diameter.

obtained by an analogous method of optical slicing and led the authors to the conclusion of unevenly distributed functional sites in the polymer bead.^[18, 23] As these findings are in contradiction to common assumptions in solid-supported chemistry they deserved further critical examination.

Employing Lambert–Beer's law the radial light intensity $I(r)$ in resin beads was calculated [Eq. (1)].^[24] Beads loaded with 1 mmol g⁻¹ of CTMR and a swelling of 5 mL g⁻¹ give a concentration c of 0.2 M. With a molar extinction coefficient (ϵ) of 10⁵ M⁻¹ cm⁻¹ the light intensity inside the bead $I(r)$ is reduced after 1 µm to 10⁻² of the initial intensity (I_0) and after 10 µm to 10⁻²⁰. Consequently, the dark interior observed by optical slicing of whole beads can be explained by the absorption of light.

$$A(r) = -\log \frac{I(r)}{I_0} = \epsilon cr; \quad I(r) = I_0 \cdot 10^{-\epsilon cr} \quad (1)$$

Optical properties of the beads such as refraction, scattering, or fluorescence quenching might also influence the detection of fluorescence from their interior. To confirm our assumption, the same resin loaded with CTMR as visualized in Figure 1 a using optical slicing was subjected to microtome-slicing. The accuracy of the slicing as well as the thickness and diameter of the slices could be determined by confocal microscopy (Figure 1 c,d). Slices of 5 µm thickness were placed on microscope slides and inspected with confocal and non-confocal fluorescence microscopy. Resin slices loaded

with 1 equiv of CTMR emitted fluorescence homogeneously from the entire sliced plane, from the outer rim as well as from the inner core (Figure 2 a).

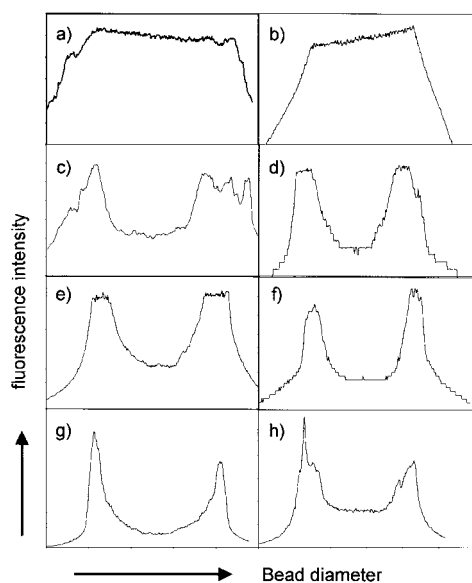


Figure 2. Intensity profiles of physical resin slices as recorded with the epifluorescence microscope. Beads were coupled with various amounts of activated CMTR or with an activated mixture of CMTR and benzoic acid as competitor: a) 1 equiv CMTR; b) 0.02 equiv CMTR, 0.98 equiv benzoic acid; c) 0.1 equiv; d) 0.05 equiv; e) 0.025 equiv; f) 0.01 equiv; g) 0.005 equiv; h) 0.001 equiv CMTR.

Fluorescence quenching can be reduced by loading resin beads with low concentrations of CTMR. Homogeneous fluorescence was also observed when 0.02 equiv CTMR were activated together with 0.98 equiv benzoic acid or N-protected leucine as non-fluorescent competitors (Figures 2 b and 3).

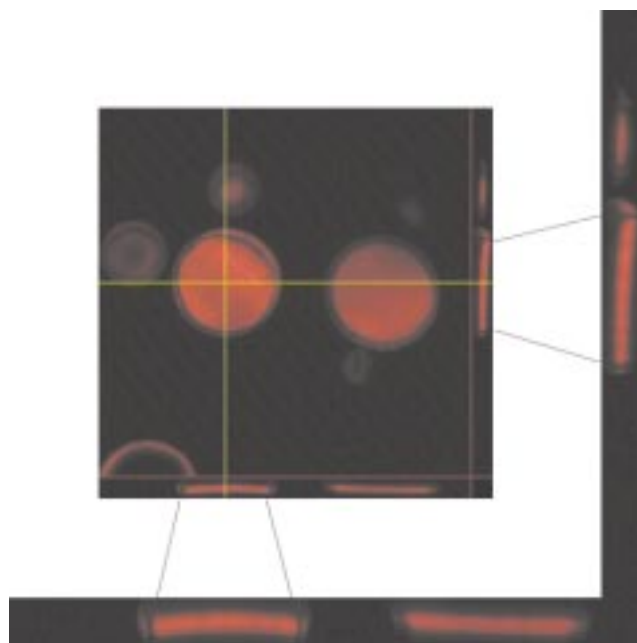


Figure 3. Confocal microscopy of two bead slices (60 μm in diameter) coupled with CTMR (0.02 equiv) and benzoic acid (0.98 equiv) as non-fluorescent competitor. Two side views along the depicted cross-sections are displayed clearly showing the homogeneous distribution of fluorophores throughout the slice.

Diffusional control of the reaction progress—The impact of the bead size: Having demonstrated the homogeneity of functional site distribution and reaction profile in rhodamine acylation, FT-IR microscopy was employed to spatially resolve the reaction progress on beads of various sizes. In the classical literature on solid-phase chemistry, an inverse correlation between bead radius and the rate constant of a reaction, which includes the formation of product gradients as well, was postulated.^[19] As this requirement is based on the diffusion characteristics of spheric reaction spaces it is valid only for reactions under diffusion control. FT-IR microscopy is suited especially for elucidating the impact of bead sizes as well as the formation of product gradients as it allows the sequential recording of the spectra of many beads and their diameters in one experiment. The generation of microtome slices is not necessary. As a typical alkylation reaction, the addition of sodium phenoxide to chloromethyl polystyrene was investigated.^[10] A mixture of chloromethyl polystyrene beads with diameters between 40 and 220 μm was treated with 1 equiv sodium 4-nitrophenolate (0.04 M) at 35 °C in DMF. The IR spectra of 50 beads were recorded at various reaction times (Figure 4 a) and the reaction progress was quantified by the ratio of the integrated nitro band at 1342 cm^{-1} and the polystyrene band at 1452 cm^{-1} (Figure 4 b). The minor differences detected in the reaction progress did not support a diffusion-controlled reaction. Several larger beads were scanned with the IR microscope as well (Figure 4 c). Homogeneous product formation across the diameter was observed. From these results we can conclude that the alkylation reaction under investigation is not diffusion-controlled on polystyrene beads, that is the reaction rate inside the beads is slow relative to the diffusion rate.

Adsorptive control in substoichiometric acylations: We finally succeeded in generating distinct product gradients in resin beads by coupling substoichiometric amounts of CTMR without competing acids (Figure 2, c–h). As mentioned above, spatial product gradients in beads possessing a homogeneous distribution of functional sites are expected in the case of a diffusion-controlled reaction. Therefore, we investigated rhodamine-diffusion out of resin beads by direct measurements. Polystyrene beads were saturated with a solution of tetramethyl rhodamine methyl ester perchlorate. The supernatant dye solution was removed by filtration. Rhodamine diffusing out of the beads was washed away by a constant flow of DMF and quantified spectrophotometrically (Figure 5). The average of repeated efflux experiments was fitted using a reported algorithm describing the diffusion out of spheric volumes [Eq. (2)].^[20]

$$n_{\text{rel}}(t) = 1 - \frac{6}{\pi^2} \sum_{i=1}^{\infty} \frac{1}{i^2} \exp\left(-\frac{D i^2 \pi^2 t}{r^2}\right) \quad (2)$$

During the first 40 s the experiment followed the diffusion model very well; the best fit was obtained for a diffusion coefficient of $10 \times 10^{-12} \text{ m}^2 \text{ s}^{-1}$ (Figure 5). Diffusion coefficients inside beads were determined for small solvent molecules by pulsed field gradient spin-echo (PGSE)

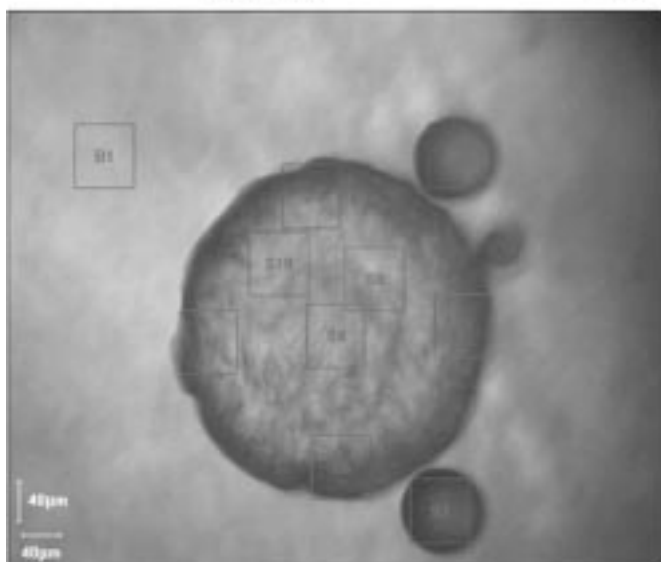
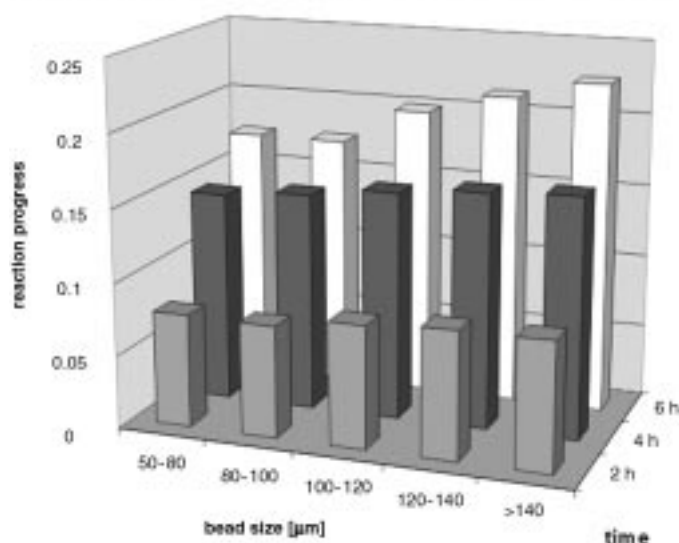
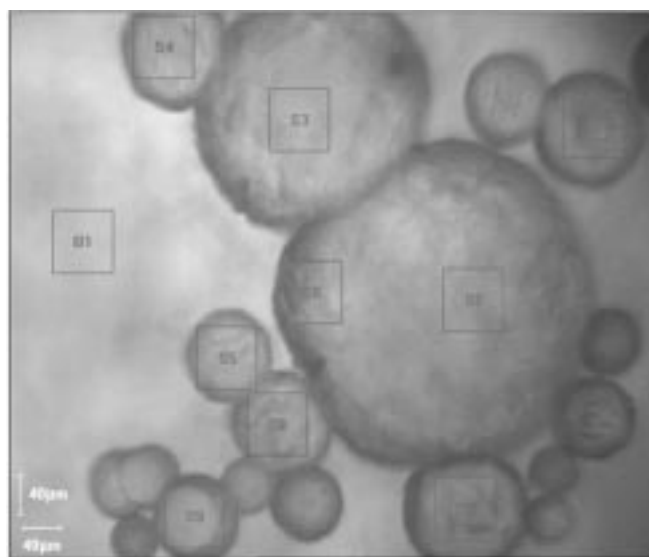


Figure 4. The progress of an alkylation reaction was studied for polystyrene beads of various sizes by FT-IR microscopy (top). Reaction progress at three reaction times was determined as the ratio of the 1342 cm^{-1} band (nitro group) and the 1452 cm^{-1} band (polymer) (middle). FT-IR microscopy was employed as well for the investigation of homogeneity in large beads (bottom).

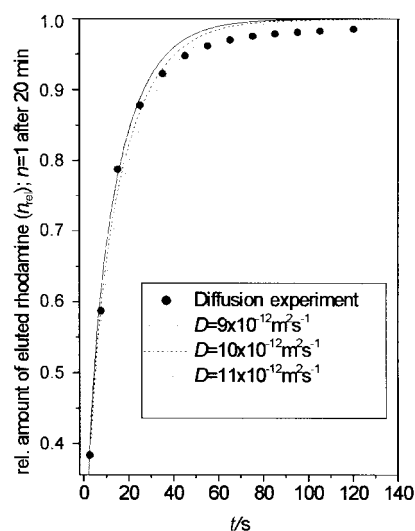


Figure 5. Averaged diffusion of rhodamine out of saturated resin beads (0.065 M). The experimental data are simulated by a diffusion algorithm for $D=9$, 10 , and $11 \times 10^{-12}\text{ m}^2\text{ s}^{-1}$. [See Eq. (2) and Supporting Information].

NMR^[21] and magnetization transfer (MT) NMR^[22] and were two orders of magnitude faster than the one of tetramethyl rhodamine measured in our experiments. The half-life of bulk diffusion was below 10 s, significantly less than the half-lives of typical acylation reactions at low concentrations.^[7] Thus, the observed product gradients were not formed by diffusion control. However, in contradiction to the diffusion model, significantly prolonged washing ($>30\text{ min}$) was required in order to remove the last 2% of rhodamine. The observed effect can be explained as rhodamine adsorption inside the resin beads. Strictly speaking the concept of adsorption is specific for solid–liquid interfaces, not for swelling polymers. However, the effect observed resembles adsorption in several respects. The removal of rhodamine by prolonged washing indicates reversibility. Secondly, the amount of rhodamine adsorbed inside the resin beads is a function of the initial dye concentration. Consequently, the product gradients observed were formed as a result of the adsorption of reactants inside the polymer. To our knowledge, these experiments constitute the first direct measurements of adsorptive effects inside swelling polymer beads. It should be emphasized, that adsorptive effects are of considerable practical relevance to solid-phase supported chemistry as they not only influence the reaction progress but determine the efficiency of washing procedures that can be crucial for efficient automatization of synthetic protocols.

Conclusion

In summary, single bead analysis by confocal and non-confocal fluorescence microscopy as well as by FT-IR microscopy demonstrates that the employed standard polystyrene beads are homogeneously functionalized. In two representative solid-phase reactions, an acylation and a nucleophilic substitution reaction, the spatially resolved reaction progress was examined as a function of the bead size and the

equivalents of reactants. Our results indicate that both solid-phase reactions were not diffusion-controlled under the conditions reported and that the bead size had no significant impact on the reaction progress. The spatial distribution of products inside polymer beads could be monitored with fluorescence as well as with IR microscopy. Product gradients were generated by employing sub-stoichiometric amounts of reactants and are formed as a result of the adsorption of reactants to the polymer as indicated by prolonged washing experiments.

Furthermore, the results indicate that physical slicing of the beads is necessary to generate realistic representations of the distribution of fluorescent dyes inside a polystyrene bead by fluorescence microscopy.

Experimental Section

General procedures: Aminomethyl divinylbenzene (1%)–polystyrene was obtained from Rapp Polymere, Tübingen, Germany, chloromethyl divinylbenzene (1%)–polystyrene was obtained from Nova Biochem AG, Läufelingen, Switzerland. DMF was purchased in HPLC grade. All reactions were carried out in plastic syringes equipped with Teflon filters.

Acylation reactions: Aminomethyl polystyrene (10 mg, 200–400 mesh, 1.00 mmol g⁻¹ loading) was treated with 5,6-carboxy-tetramethylrhodamine (CTMR) (1, 0.1, 0.05, 0.025, 0.01, 0.005, or 0.001 equiv), tetramethyl-*O*-(benzotriazol-1-yl)-uronium tetrafluoroborate (TBTU), and *N*-diisopropylethyl amine (Hünigs Base) (both equimolar with respect to CTMR) in DMF (1 mL). Alternatively, a mixture of CTMR (0.02 equiv) with benzoic acid (0.98 equiv) or *N*-protected leucine (0.98 equiv) as non-fluorescent competitor was activated as described and employed. After 20 h the resins were washed with DMF (10 ×) and with THF, CH₂Cl₂, and methanol (5 ×) and were dried in vacuo for 16 h.

Alkylation reactions: Chloromethyl polystyrene resins with various bead sizes (33 mg of 70–90 mesh with 1.26 mmol g⁻¹ loading, 33 mg of 100–200 mesh with 1.20 mmol g⁻¹ loading, and 33 mg of 200–400 mesh with 1.20 mmol g⁻¹ loading) were combined in one syringe. A solution of sodium 4-nitrophenolate (0.04 M, 1 equiv) in DMF was added to the resin mixture and the reaction mixture was allowed to react at 35 °C. After 2 h, 4 h, and 6 h, respectively, a small fraction was removed from the mixture and washed with DMF (10 ×) and water, DMF, THF, CH₂Cl₂, and methanol (each 5 ×). The resin fractions were dried in vacuo. A few beads of each sample were placed on a prefabricated KBr pellet and carefully pressed into the pellet employing a metal piston. This procedure assured to obtain IR spectra of improved quality.

Microtome slicing: A rectangular mould was placed on a microscope slide. A few millimeters of molten paraffin were added. CTMR-labelled beads were distributed evenly on the paraffin surface and the mould was filled with paraffin. After cooling the mould was removed. Slices of 5 μm thickness were obtained employing a Leica microtome and placed on microscope slides. The paraffin was removed by subsequent treatment with toluene (3 ×, 10 min), isopropanol (2 ×, 5 min), 96% isopropanol (2 ×, 5 min) and 70% isopropanol (5 min).

Confocal fluorescence microscopy: Confocal fluorescence microscopy was conducted employing a Zeiss LSM 510 laser scanning microscope. Excitation at 543 nm was effected using a He/Ne laser. Swollen as well as non-swollen beads were examined. For the measurements of the swollen beads a drop of DMF or water was added to the beads on the microscope slide and a cover slip was placed on top. The measurements of the non-swollen beads were carried out without covering of the slide.

Fluorescence microscopy: Fluorescence microscopy (non-confocal) was conducted with an Axiovert 100 M epifluorescence microscope. Excitation of the fluorescence was effected by an Osram HBO 50 mercury lamp. Pictures were recorded with a PCO Sencam Super VGA camera. For all measurements a 40 × 0.75 objective was used. With the epifluorescence microscope only non-swollen beads were examined.

IR microscopy: All spectra were recorded on a BIO-RAD FTS-135 spectrometer coupled with a UMA 500 IR microscope, using a SPC-3200 data station. The microscope is equipped with a liquid nitrogen cooled mercury/cadmium/telluride (MCT) detector. In the view mode (visible light) the total magnification is 150 ×, which enabled the location and size determination of individual beads. IR spectra were recorded in the transmission mode. Data were collected with a resolution of 4 cm⁻¹, 100 scans for the beads and 25 scans for the background measurements were averaged. All spectra were analyzed by integrating the typical band of polystyrene at 1452 cm⁻¹ and the nitro band at 1342 cm⁻¹. The ratio of these two bands were correlated with the diameter of the bead and the reaction time. For each sample 50 spectra were analyzed. The results are plotted in Figure 4.

Diffusion studies: Chloromethyl polystyrene beads (6 mg, 200–400 mesh) were exposed to a solution of tetramethylrhodamine methyl ester perchlorate in DMF (0.065 M, 100 μL) for 20 h. The supernatant dye solution was removed by filtration. The beads were washed in a continuous flow of DMF (0.5 mL min⁻¹) by employing a syringe pump. The eluent solution was collected in intervals (10 s) and the eluted rhodamine was quantified spectrophotometrically. The molar extinction coefficient at 559 nm (110933 M⁻¹ cm⁻¹) was determined by a six-point calibration. The diffusion was simulated for various diffusion coefficients ($D = 9, 10, \text{ and } 11 \times 10^{-12} \text{ m}^2 \text{ s}^{-1}$) employing a diffusion algorithm for spherical volumes [ref. [20], p. 91, Equation (6.20)]. For the calculation a visual basic program was used; calculations were conducted for an average bead radius of 40 μm observed for beads swollen in DMF (Figure 5). Good agreement of the simulation with the experimental data was only observed for the first 40 s of the experiment. The best fit was found for a diffusion coefficient of $10 \times 10^{-12} \text{ m}^2 \text{ s}^{-1}$. Contrary to the diffusion equation, washing for >30 min was required to restore almost colorless beads. After 70 s the simulated diffusion is already completed, whereas a significant amount of rhodamine (1.7 mmol g⁻¹) remained adsorbed inside the beads.

Acknowledgement

We thank Dr. Peter Ruck, Institute of Pathology, University of Tübingen, for preparing the microtome slices. J.R. gratefully acknowledges the support from Prof. M. E. Maier, Tübingen, from the Strukturfonds of the University of Tübingen and the DFG. We thank the DFG-Graduiertenkolleg "Chemistry in Interphases" from which M.B. receives a graduate fellowship and Merck KgaA, Darmstadt, Germany, for support. R.B. is a recipient of a postdoctoral fellowship from the Volkswagen Foundation.

- [1] *Combinatorial Chemistry—Synthesis, analysis, screening* (Ed.: G. Jung), Wiley-VCH, Weinheim, 1999.
- [2] *Combinatorial peptide and nonpeptide libraries* (Ed.: G. Jung), VCH, Weinheim, 1996.
- [3] D. C. Sherrington In *Polymer-supported reactions in organic synthesis* (Eds.: P. C. Hodge, D. C. Sherrington), Wiley, Chichester, 1980, p. 1–82.
- [4] D. C. Sherrington, *Chem. Commun.* 1998, 2275–2286.
- [5] M. Meldal In *Solid Phase Peptide Synthesis* (Ed.: G. Fields), Academic Press, New York, 1998, p. 83–104.
- [6] D. Hudson, *J. Comb. Chem.* 1999, 1, 333–360; D. Hudson, *J. Comb. Chem.* 1999, 1, 402–457.
- [7] W. Li, B. Yan, *J. Org. Chem.* 1998, 63, 4092–4097.
- [8] W. Li, X. Xiao, A. W. Czarnik, *J. Comb. Chem.* 1999, 1, 127–129.
- [9] M. Pursch, G. Schlotterbeck, L.-H. Tseng, K. Albert, W. Rapp, *Angew. Chem.* 1996, 108, 3034–3036; *Angew. Chem. Int. Ed. Engl.* 1996, 35, 2867–2869.
- [10] W. J. Haap, T. B. Walk, G. Jung, *Angew. Chem.* 1998, 110, 3503–3505; *Angew. Chem. Int. Ed. Engl.* 1998, 37, 3311–3314.
- [11] R. B. Merrifield, V. Littau In *Peptides 1968* (Ed.: E. Bricas), North-Holland, Amsterdam, 1968, p. 179–182.
- [12] V. S. Sarin, S. B. H. Kent, R. B. Merrifield, *J. Am. Chem. Soc.* 1980, 102, 5463–5470.
- [13] J. Rademann, M. Groetli, M. Meldal, K. Bock, *J. Am. Chem. Soc.* 1999, 121, 5459–5466.
- [14] J. Rademann, G. Jung, *Science* 2000, 287, 1946–1947.

- [15] J. N. Turner, W. Shain, D. H. Szarowski, S. Lasek, N. Dowell, B. Sipple, A. Can, K. Al-Kofahi, B. Roysam, *J. Histotechn.* **2000**, *23*, 205–217.
- [16] P. Shaw, *Histochem. J.* **1994**, *26*, 687–694.
- [17] B. Fleckenstein, K.-H. Wiesmüller, M. Brich, G. Jung, *Lett. Pept. Sci.* **1994**, *1*, 117–126.
- [18] S. R. McAlpine, S. L. Schreiber, *Chem. Eur. J.* **1999**, *5*, 3528–3532.
- [19] F. Helfferich, *Ion Exchange*, McGraw-Hill, New York, **1962**.
- [20] J. Crank, *The Mathematics of Diffusion*, 2nd ed., Clarendon, Oxford, **1975**.
- [21] S. Pickup, F. D. Blum, J. G. Ford, M. Periyasamy, *J. Am. Chem. Soc.* **1986**, *108*, 3987–3990.
- [22] W. T. Ford, B. J. Ackerson, F. D. Blum, M. Periyasamy, S. Pickup, *J. Am. Chem. Soc.* **1987**, *109*, 7276–7280.
- [23] S. R. McAlpine, C. W. Lindsley, J. C. Hodges, D. M. Leonard, G. F. Filzen, *J. Comb. Chem.* **2001**, *3*, 1–5.
- [24] A. Liljeborg, *SPIE* **1996**, 2655, 11–17.

Received: December 8, 2000 [F 3084]